Cholinergic mesencephalic neurons are involved in gait and postural disorders in Parkinson disease.

Carine Karachi, David Grabli, Frédéric A. Bernard, Dominique Tandé, Nicolas Wattiez, Hayat Belaid, Eric Bardinet, Annick Prigent, Hans-Peter Nothacker, Stéphane Hunot, et al.

Cholinergic mesencephalic neurons are involved in gait and postural disorders in Parkinson disease

Carine Karachi,[1,2,3,4] David Grabli,[1,2,3,4] Frédéric A. Bernard,[1,2,3,5] Dominique Tandé,[1,2,3] Nicolas Wattiez,[1,2,3] Hayat Belaid,[1,2,3,4] Eric Bardinet,[1,2,3] Annick Prigent,[1,2,3] Hans-Peter Nothacker,[6] Stéphane Hunot,[1,2,3] Andreas Hartmann,[1,2,3,4] Stéphane Lehéricy,[1,2,3] Etienne C. Hirsch,[1,2,3] and Chantal François[1,2,3]

[1]Université Pierre et Marie Curie — Paris 6, CR-ICM, UMR-S975, Paris, France. [2]INSERM, U975, Paris, France. [3]CNRS, UMR 7225, Paris, France. [4]Assistance Publique-Hôpitaux de Paris, Groupe Pitié-Salpêtrière, Paris, France. [5]Laboratoire d'Imagerie et de Neurosciences Cognitives, FRE 3289, CNRS/Université de Strasbourg, Strasbourg, France. [6]Department of Pharmacology, School of Medicine, University of California, Irvine, California, USA.

Gait disorders and postural instability, which are commonly observed in elderly patients with Parkinson disease (PD), respond poorly to dopaminergic agents used to treat other parkinsonian symptoms. The brain structures underlying gait disorders and falls in PD and aging remain to be characterized. Using functional MRI in healthy human subjects, we have shown here that activity of the mesencephalic locomotor region (MLR), which is composed of the pedunculopontine nucleus (PPN) and the adjacent cuneiform nucleus, was modulated by the speed of imagined gait, with faster imagined gait activating a discrete cluster within the MLR. Furthermore, the presence of gait disorders in patients with PD and in aged monkeys rendered parkinsonian by MPTP intoxication correlated with loss of PPN cholinergic neurons. Bilateral lesioning of the cholinergic part of the PPN induced gait and postural deficits in nondopaminergic lesioned monkeys. Our data therefore reveal that the cholinergic neurons of the PPN play a central role in controlling gait and posture and represent a possible target for pharmacological treatment of gait disorders in PD.

Introduction

Gait disorders and postural instability represent a major burden in the elderly population and are commonly observed in severe and advanced forms of Parkinson disease (PD; ref. 1). While most parkinsonian symptoms can be alleviated by L-dopa replacement therapy, gait disorders respond poorly to dopaminergic drugs, which suggests that they are caused by nondopaminergic lesions.

Despite our current knowledge of the basic physiology of gait, the alterations in the central nervous system that cause gait disorders have yet to be identified. Experimental studies have revealed that the optimal site for the induction of rhythmic stepping behavior in decerebrate animals lies in a functionally defined mesencephalic locomotor region (MLR). Anatomically, the MLR encompasses the cuneiform nucleus (2) and the pedunculopontine nucleus (PPN), which is heterogeneously composed of cholinergic and noncholinergic neurons (3). Whether these structures are involved in human gait is still under debate, given the inconsistent results of functional MRI (fMRI) studies using mental imagery of gait to model real gait (4–6). In PD, among the different nondopaminergic neuronal systems affected (7), cholinergic cell loss was found in the PPN of patients with the most severe dopaminergic degeneration (8). Based on the assumption that gait failure is induced by PPN lesion or dysfunction (9), recent therapeutic trials tested the efficacy of electrical modulation of the PPN in reducing these symptoms in selected parkinsonian patients (10–14). However, the variability of the results raised doubts about the initial hypothesis and emphasized the need to determine the role of the PPN, in particular its cholinergic part, in gait and posture.

In the present study, using a broad range of approaches in humans and monkeys in either the normal or the parkinsonian state, we demonstrated that the PPN, and more particularly its cholinergic part, is essential in controlling the performance of gait and posture.

Results

The PPN region is activated during fast imagined walking in healthy humans. Since PPN neurons are reported to increase their firing rate in response to step frequency in human parkinsonian patients (15), we hypothesized that the activity of the PPN region could be modulated by the speed of imagined gait. To address this issue, we performed an fMRI study in healthy subjects using a modified version of a previously validated paradigm (5). The subjects were instructed to perform an imagery of gait (IG) task at either normal or faster speed, based on the assumption that imaginary movement and actual movement execution activate overlapping areas (15). Imagery of object movement (IOM) was used as a control task; subjects were asked to imagine a disk moving in the same environment at either normal or faster speed (at around 30% faster). To ensure that the subjects had performed the tasks properly, we first measured imagery times required to perform the task, and verified that the faster the speed, the shorter the imagery time (Supplemental Figure 1; supplemental material available online with this article; doi:10.1172/JCI42642DS1). The comparison between the IG and IOM conditions yielded significant activations in a network of brain regions that include the superior frontal gyri and the cingulate cortex (Figure 1A and Table 1), as previously described (5). As expected, the comparison between the faster IG and normal IG conditions revealed substantial activation of a single cluster in the MLR in the left midbrain (Figure 1B). Superimposed anatomical structures revealed

Authorship note: Carine Karachi and David Grabli contributed equally to this work.
Conflict of interest: The authors have declared that no conflict of interest exists.
Citation for this article: *J Clin Invest.* 2010;120(8):2745–2754. doi:10.1172/JCI42642.

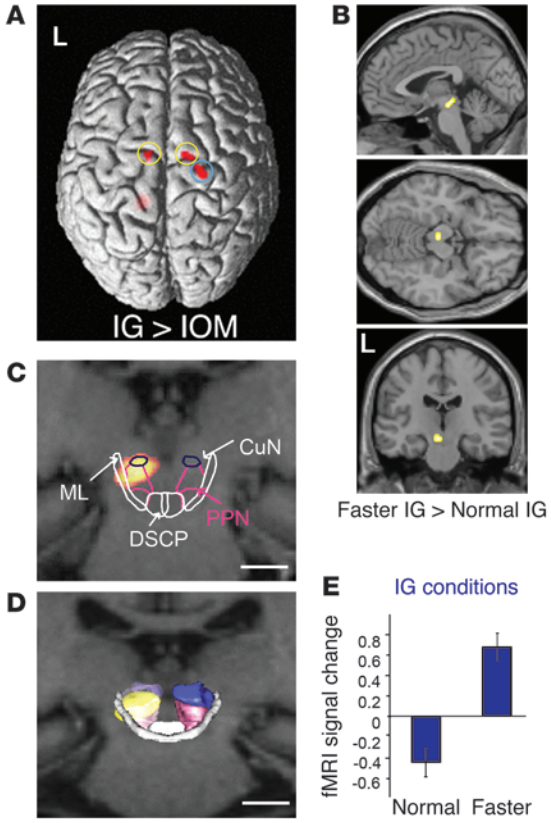

Figure 1
Cerebral activity during IG and IOM in 15 healthy volunteers. (**A**) Regions of significant activation superimposed on a rendered brain viewed from above, showing increased activity in the superior frontal gyrus bilaterally (yellow circles) and the right precentral gyrus (blue circle) for the comparison of IG versus IOM ($P < 0.001$, uncorrected for multiple comparisons; cluster size, >30 voxels). (**B**) Regions of significant activation superimposed on T1-weighted images (top, sagittal; middle, transverse; bottom, coronal), showing increased activity in the left PPN and cuneiform nucleus for the comparison of faster versus normal IG ($P < 0.001$, uncorrected for multiple comparisons; cluster size, >30 voxels). Activity in this region survived a small volume correction (10-mm radius) for multiple comparisons (family-wise error, $P < 0.05$). (**C**) Regions of significant activation, superimposed on the tracing of cerebral contours in the PPN region, in a coronal MRI section. (**D**) Posterior view of the PPN and cuneiform nucleus. (**E**) Plots of activity in left PPN and cuneiform nucleus (x, –3; y, –22; z, –13) for normal and faster IG conditions. For t values of each contrast, see Table 1. CuN, cuneiform nucleus; DSCP, decussation of superior cerebellar peduncle; L, left; ML, medial lemniscus. Scale bars: 10 mm.

that this cluster included the PPN and the adjacent cuneiform nucleus (Figure 1, C and D). Therefore, the PPN and cuneiform nucleus were activated during fast IG.

Cholinergic neurons in the PPN degenerate in faller PD patients. Freezing of gait and postural instability are often encountered in severe and advanced forms of PD. Because several lines of evidence suggest that these symptoms may be related to the degeneration of cholinergic neurons within the PPN, we determined whether neuronal loss in this structure was more severe in PD patients with balance deficits and falls than in PD patients without them. Using stereology, we quantified the number of cholinergic neurons labeled for acetylcholinesterase (AChE) histochemistry on 5 anteroposterior, regularly interspaced PPN sections (Figure 2, A and B) in 3 groups of human brains: healthy controls ($n = 8$), PD patients without balance deficits or falls (nonfaller PD; $n = 6$), and PD patients with balance deficits and falls (faller PD; $n = 6$). The number of AChE$^+$ neurons in faller PD patients was significantly lower than in nonfaller PD patients (609 ± 61 vs. 934 ± 63 neurons; $P < 0.01$, Kruskall-Wallis test followed by Mann-Whitney U test) and in controls (1,058 ± 52 neurons; $P < 0.01$; Figure 2C). The number of Nissl-stained neurons in the adjacent cuneiform nucleus, as measured by stereology, was not significantly different ($P = 0.59$, Mann-Whitney U test) between faller PD patients (3,502 ± 567 neurons/mm^3; 31% loss compared with controls) and nonfaller PD patients (3,152 ± 241 neurons/mm^3; 38% loss compared with controls). As expected, the number of tyrosine hydroxylase–positive (TH$^+$) neurons in the substantia nigra, as quantified by stereology, was severely reduced in both PD groups compared with controls (faller PD, 32,495 ± 4,799 neurons; nonfaller PD, 80,478 ± 30,968 neurons; control, 260,955 ± 19,482 neurons; $P < 0.01$, Mann-Whitney U test; Figure 2D). Interestingly, the loss of dopamine neurons was also significantly more severe in faller than in nonfaller PD patients ($P < 0.01$, Kruskall-Wallis test followed by Mann-Whitney U test).

A loss of cholinergic neurons is detected in the PPN of aged parkinsonian monkeys displaying balance deficits. The current monkey models of PD are developed using 1-methyl-4-phenyl-1,2,3,6-tetrahydropyridine (MPTP), a selective neurotoxin that produces dopamine depletion but no loss of PPN cholinergic neurons in young adult monkeys (16, 17). Yet, because aged but not young monkeys develop balance and postural deficits after intoxication with MPTP (18), we tested the possibility that these symptoms are associated with a loss of cholinergic neurons in the PPN. Young and aged MPTP-treated monkeys (total $n = 8$) developed motor symptoms (akinesia, rigidity, and episodes of tremor). Young MPTP-treated monkeys ($n = 4$) scored 10–12 on a disability scale of 0–25 (18), with no balance or posture deficits. In contrast, aged MPTP-treated monkeys ($n = 4$) developed a more severe parkinsonism, with scores ranging between 14 and 19 on the disability scale, and displayed major balance deficits and abnormal postures, as previously reported (19). To identify neuronal correlates of these differences, we analyzed nigral dopaminergic neurons and cholinergic neurons in PPN following sacrifice of the animals. Both groups of MPTP-treated animals displayed a dramatic loss of dopaminergic neurons in the substantia nigra and of dopaminergic fibers in the striatum (Supplemental Figure 2). In the aged MPTP-treated monkeys, the density of TH$^+$ fibers, as quantified by optical density measurements, showed a significant decrease of 90% in the caudate nucleus and 95% in the sensorimotor putamen compared with the controls. In the young animals, the decreases were 93% and 96%, respectively. PPN cholinergic neurons were then identified by NADPH diaphorase histochemistry (Figure 3A), which selectively labels these neurons in the PPN (18). They were quantified by stereology on 5 anteroposterior, regularly spaced sections throughout the PPN. The total number of NADPH$^+$ neurons did not differ between young and aged monkeys (young, 1,038 ± 18 neurons; aged, 885 ± 55 neurons; Figure 3B). In contrast, whereas MPTP did not affect the number of NADPH$^+$ neurons in young animals (949 ± 33 neurons), it induced a 30% loss of cholinergic neurons in aged monkeys (600 ± 19 neurons; $P < 0.01$, Mann-Whitney U test).

Table 1
Group analysis of the network activated during IG relative to IOM and faster versus normal gait

Brain region	Side	BA	Stereotactic coordinate			*t* value
			x	*y*	*z*	
IG versus IOM						
Superior frontal gyrus	L	6	–11	–6	67	4.17
Superior frontal gyrus	R	6	13	–8	78	4.12
Precentral gyrus	R	6	21	–18	69	4.16
Median cingulate and paracingulate gyri	L	23	–16	–38	32	5.49
Cerebellum	R		5	–46	–42	5.12
Faster IG versus normal IG						
Pedunculopontine and cuneiform nuclei	L		–3	–22	–13	6.11

Shown are significant signal increases in various brain regions ($P < 0.001$, uncorrected, cluster size >30) for IG versus IOM and faster IG versus normal IG. Stereotactic coordinates are reported in MNI space. BA, Brodmann area; L, left; R, right.

Because microglia may contribute to changes in normal aging, we analyzed the microglial reaction in the PPN of our young and aged normal monkeys. An increased number of microglial cells stained for HLA-DR antigen was detected in aged compared with young monkeys (2.4 ± 0.3 versus 1.5 ± 0.2 cells/mm^3; $P < 0.01$, Mann-Whitney *U* test).

Cholinergic lesion within the PPN induces gait and postural disorders. Since the PPN was activated in the IG task in healthy humans, and since PPN cholinergic lesion was associated with gait disorders in both human disease and the monkey model of PD, we sought to demonstrate experimentally that PPN cholinergic lesion without dopaminergic injury is sufficient to induce a gait deficit. Bilateral injections of urotensin II–conjugated diphtheria toxin (3–10 μl, 20%–30%) in the PPN of 5 animals resulted in significant and reproducible changes in gait and posture during the 7–8 weeks of survival. These symptoms included a decrease in the angle of the knee and in step length and speed, an increase in the back curve, deviation of the hindquarters and of the head, modification of the tail position (axial rigidity), and arm and leg rigidity (Figure 4 and Table 2). Importantly, no modification of global motor activity in the home cage was detectable, except for animal M2. None of these gait and postural parameters improved after injection of 120 μg/kg apomorphine (Figure 4), which confirmed that they were unrelated to dopamine depletion.

Cholinergic neurons of the PPN were then studied postmortem by NADPH diaphorase histochemistry (Figure 5B). Mapping of the injection sites (Figure 5C) revealed that even though the loss of cholinergic neurons was variable from one monkey to another, all injection sites were located within the cholinergic part of the PPN in all animals (Figure 5D). The number of NADPH$^+$ neurons was reduced by a mean of 39% in the lesioned animals compared with controls (PPN-lesioned, 4,951 ± 621 neurons, $n = 5$; control, 8,178 ± 236 neurons, $n = 5$; $P < 0.01$, Mann-Whitney *U* test; Figure 5E). Moreover, we also determined that myelinated fibers were preserved after the toxin injections (Figure 5F).

Comparison of gait and posture disorders between MPTP-induced dopaminergic injury and PPN lesion. We then compared bilateral PPN lesion–induced gait and walking disorders with those induced by the dopaminergic depletion caused by MPTP injection. The most prevalent symptom observed in the 4 MPTP-treated macaques was akinesia, assessed on the basis of a dramatic and significant decrease in global activity in the home cage, in arm speed during a food retrieval task, and in step speed during locomotion (Figure 4). The animals also displayed a cog-wheel rigidity of the extremities, characteristic of the parkinsonian state and unlike the rigidity observed in monkeys with PPN lesion. Gait and posture deficits observed in the MPTP-treated macaques included a decrease in step length and speed and an increase in the back curve, as in monkeys after PPN lesion. However, the major difference between the 2 groups was that in MPTP-treated animals, these symptoms were significantly reversed by apomorphine treatment (Figure 4).

Discussion

Identifying the brain structures involved in gait and balance and elucidating their dysfunction are prerequisites for the development of new treatments designed to reduce the occurrence of falls in the elderly, a major public health and community problem. Our study is the first to our knowledge to demonstrate that gait and posture in primates are under the control of cholinergic neurons of the PPN. This statement is based on converging evidence from (a) an fMRI study that showed increased activation of the MLR, and more particularly the PPN, during fast compared with normal IG in healthy human subjects and (b) an experimental study showing that lesion of the cholinergic neurons of the PPN was sufficient to produce gait and posture deficits in normal monkeys. In addition, we found a correlation between the loss of PPN cholinergic neurons and balance deficits in the parkinsonian state and in aged MPTP-treated monkeys. This result helps to clarify the pathophysiology of L-dopa–resistant deficits of gait and posture in advanced forms of PD and highlights the key role of a PPN cholinergic lesion in these symptoms.

One of the main findings of our study was that PPN lesion induced gait deficits. This is in line with previous experimental studies showing that electrical or pharmacological manipulations of the PPN region can modulate gait on a treadmill in decerebrate cats and rodents (2, 20, 21). In these experiments, increasingly higher levels of electrical stimulation of the PPN region drove the frequency of stepping from a walk to a gallop (22), which suggests that the activation level of the PPN area is critical for the cadence of gait. This is consistent with our fMRI results obtained in healthy humans during IG, in which the PPN region was activated after an increase in the speed of gait. Likewise, extracellular recordings of the PPN region obtained in human parkinsonian patients showed that neurons increase their firing rate according to step frequency (15). Conversely, PPN activation could be related to higher-order functions, such as the visuospatial or attentional processes needed to maintain a certain level of motor performance in faster gait. Experimental data in rodents suggest that the PPN establishes high-order function rather than basic motor control (23). In line with this concept, the axial deficits observed in the present study after specific cholinergic lesion of the PPN were surprising, since they contrast with previous results obtained after experimental lesion of the PPN without discrimination of targeted neuronal subtypes as performed with ibotenic lesions in rats. These ibo-

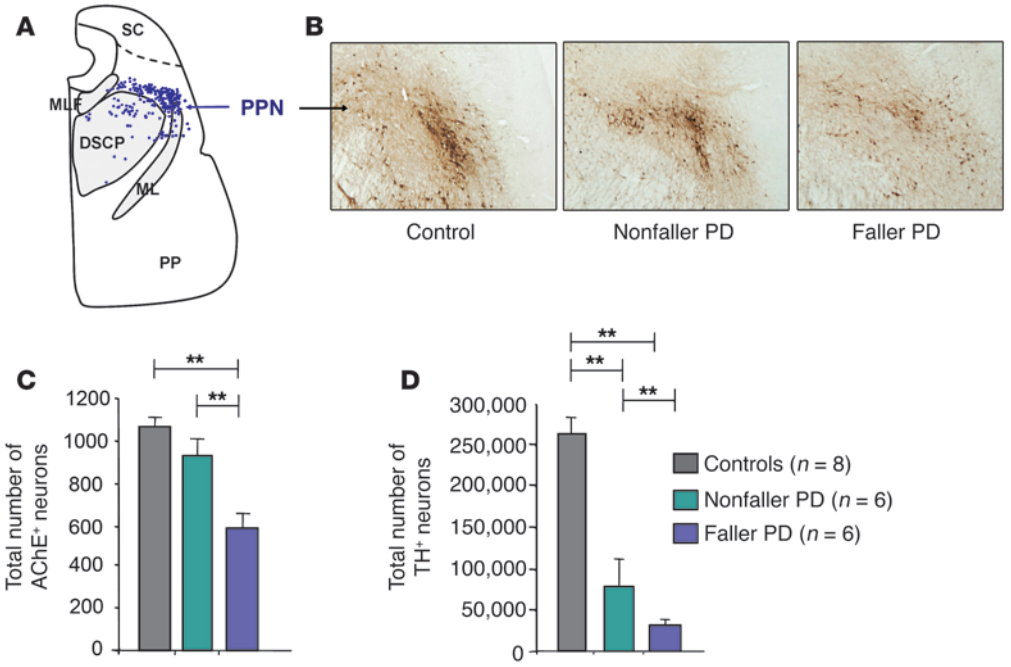

Figure 2

Relationship between loss of PPN cholinergic neurons and balance deficits in human PD patients. (**A**) Computer-generated map of AChE+ neurons in the PPN of a control brain. Blue dots represent individual neurons. (**B**) Transverse sections at PPN level illustrating that the loss of AChE+ neurons of a faller PD patient was more severe than in a nonfaller PD patient. (**C**) Total number of AChE+ neurons in the PPN of controls ($n = 8$), nonfaller PD patients ($n = 6$), and faller PD patients ($n = 6$). The mean value for the faller PD patients was significantly different from the mean for the control group and from the mean for the nonfaller PD patients. (**D**) Total number of TH+ neurons in the substantia nigra pars compacta of the same groups of control and PD patients. The mean values for the 2 PD groups were significantly different from the mean for the control group. MLF, medial longitudinal fasciculus; PP, pes pedunculi; SC, superior colliculus. $^{**}P < 0.01$, Mann-Whitney *U* test. Scale bar: 1 mm.

tenic PPN lesions resulted in subtle cognitive deficits, but failed to induce impairment in spontaneous locomotion (24, 25), except for a deficit in baseline activity when the lesion involved the anterior PPN (26). In monkeys, PPN lesion induced typical parkinsonism with akinesia and hypertonia, but the behavioral analysis in the previous studies did not focus on gait and posture (27–29). In this context, it is intriguing that the PPN lesions we performed in monkeys failed to produce akinesia. These discrepancies could be related to the subtype of injured neurons or to the size of the lesions. Indeed, in previous studies in primates, the lesions were made using kainate, an excitotoxin not specific to a particular neuronal population that produces strong seizures and very large lesions. Therefore, it is quite possible that some structures adjacent to the PPN also participated in the development of akinesia and hypertonia. Moreover, in the previous studies, primate behaviors were tested during the first 7 postoperative days, when excitotoxin had seizure-promoting activity (30), but not later. In contrast, the PPN lesions made in our macaques selectively targeted a small population of neurons and were not sufficient to produce akinesia, but were large enough to induce clear postural and gait deficits that persisted until 7 weeks after surgery.

The large cluster of activation that we detected in the left PPN region of right-handed healthy subjects during fast imagined walking suggests the dominance of this left brainstem region for the locomotor system. In support of this view, a further comparison between the faster and normal IG conditions with a more lenient threshold ($P < 0.005$, uncorrected) highlighted an additional activation located in the left supplementary motor area (x, –8; y, –2; z, 54), which is the repository of the dominant right leg representation and is connected to the left PPN. This left dominance is in line with previous studies demonstrating that certain higher motor functions, such as execution of movement sequences, might be controlled more by the left hemisphere than by the right for both left- and right-limb movements (31, 32).

The postural and gait deficits that we observed after PPN lesions may partially resemble those obtained after dopaminergic denervation, since they share common features, such as rigidity, reduction of step length, or stooped posture during walking. However, a cog-wheel rigidity of the limbs was a characteristic that macaques displayed only after MPTP treatment, not after PPN lesion. Moreover, results of more detailed analysis supported the conclusion that the deficits actually differed, since no improvement of the symptoms with dopamine agonist treatment were observed after PPN lesion. In summary, our data demonstrated that while the dopaminergic system participates in the control of gait and posture, the PPN cholinergic system plays a complementary role with a specific contribution for each of these 2 systems. Additional fMRI experiments comparing PPN activation in faller and nonfaller PD patients and in healthy subjects would provide further clues to the role of the PPN in axial symptoms.

A prominent finding of our study was that cholinergic neurons of the PPN were involved in gait and balance disorders. The toxin that we used preferentially targeted the cholinergic neurons of the PPN, yet because some noncholinergic neurons were also affected (Supplemental Figure 4, B and C), we cannot

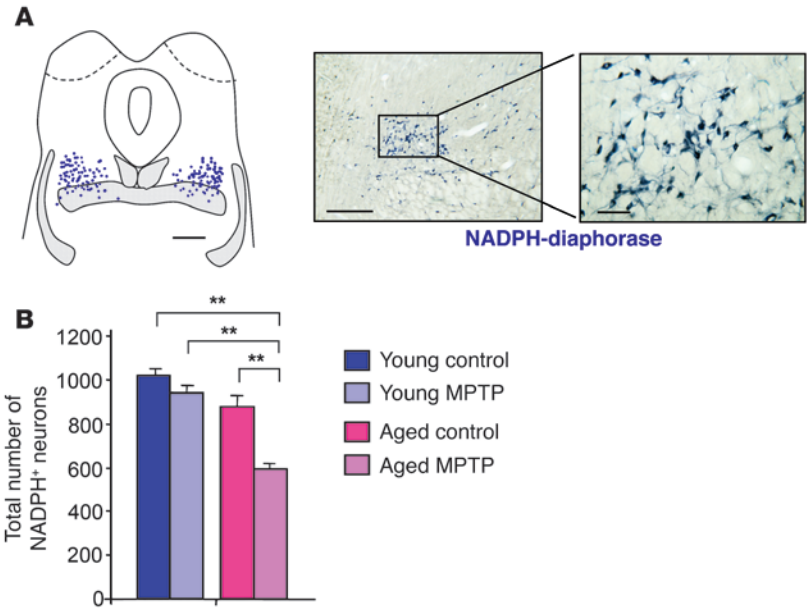

Figure 3
Loss of PPN cholinergic neurons in MPTP-treated macaques. (**A**) NADPH+ neurons mapped in the PPN of a control brain of a young macaque; hatched areas denote myelinated nerve fibers in the brainstem and blue dots represent individual neurons. Low- and high-magnification images are shown at right. (**B**) Total number of NADPH+ neurons quantified in young and aged MPTP-intoxicated macaques compared with their respective controls ($n = 4$ per group). MPTP did not affect NADPH+ neurons in young animals, but induced a 30% loss of cholinergic neurons in aged monkeys. $^{**}P < 0.01$, Mann-Whitney U test. Scale bars: 2 mm (map); 500 μm (low magnification); 100 μm (high magnification).

entirely rule out the possibility that some symptoms may arise from a noncholinergic lesion. However, several lines of evidence from the postmortem data suggest that cholinergic lesions play a role in gait and balance disorders. Indeed, we observed a correlation between gait disorders and cholinergic neuronal loss within the PPN of PD patients. Previous studies already showed that cholinergic neuronal loss within the PPN was correlated with the level of dopaminergic degeneration (8) and with the clinical severity of the disease (33). However, to our knowledge, this is the first postmortem study in PD patients establishing a correlation between the occurrence of falls and freezing and the loss of cholinergic neurons in the PPN. We are aware that this correlation could be explained by confounding factors, such as a higher level of dopaminergic cell loss in patients with severe PPN cholinergic lesion. However, this possibility is unlikely, since the axial symptoms that we observed in the PD patients with prominent PPN cholinergic loss were not improved by dopaminergic treatment. Alternatively, the involvement of lesions in other brain structures (7) in the control of gait and posture might explain these symptoms. Nevertheless, the fact that the degree of neuronal loss in the cuneiform nucleus was not significantly different in the 2 groups of PD patients argues against the likelihood that whole-brain degeneration is more severe in faller than in nonfaller PD patients.

It is also interesting to note that PPN cholinergic neurons also degenerated in aged MPTP-treated monkeys, which develop postural and balance deficits after MPTP treatment (19). At first sight, this finding is puzzling since MPP+, the active metabolite of MPTP, is selectively taken up by dopaminergic terminals and thus does not act directly on cholinergic neurons. One possible explanation for this finding could be related to the profound atrophic changes that occur in cholinergic neurons of the PPN during aging (34, 35). An age-related increase in activated microglial cells in the PPN of aged normal monkeys, as observed in the present study, could also account for MPTP toxicity on cholinergic cells in aged MPTP-treated monkeys (36). Since PPN neurons project to nigral dopaminergic neurons (37), which, conversely, project back to PPN neurons (38), it is also possible that loss of target neurons or lack of proper dopaminergic inputs induced by MPTP treatment is added to age-related alteration of cholinergic neurons.

Finally, our findings provide a rationale for specifically targeting the cholinergic entity of the PPN as a strategy for the treatment of falls. Indeed, the direct involvement of PPN neurons in the control of gait and posture is in line with recent clinical data in PD patients showing that low-frequency electrical stimulation of the PPN area improved axial symptoms (10–14). The contribution of PPN cholinergic neurons could not have been determined previously from studies that used electrical stimulation or pharmacological manipulations. Thus, the identification of a specific subset of neurons crucially involved in postural control is of clinical significance, since better functional mapping of the PPN area may lead to the improvement of surgical targeting. Indeed, given the close proximity of the cholinergic and noncholinergic compartments within the PPN, the effects of electrical stimulation would vary according to current intensity and electrode location. Alternatively, pharmacologic manipulation of the surviving cholinergic neurons, or a strategy aimed at their protection, might represent an alternative therapeutic approach for falls in parkinsonian patients or for elderly people suffering from falls. Our results suggest that enhancing the cholinergic signal at the level of PPN targets could be a symptomatic treatment for gait failure in advanced PD. The administration of cholinesterase inhibitor would increase the efficiency of the acetylcholine released by the surviving cholinergic neurons. Yet, as observed for cognitive functions in patients with Alzheimer disease, the benefit of such manipulation would appear to be rather limited. Administration of nicotine or nicotinic agonists to act postsynaptically on cholinergic receptors might prove a more effective form of pharmacological manipulation. One of the main limitations of all these approaches is the lack of specificity of cholinergic manipulation for the PPN cholinergic system. Identification of cholinergic agonists specific to receptors expressed in the targets of cholinergic PPN neurons could also be a promising approach.

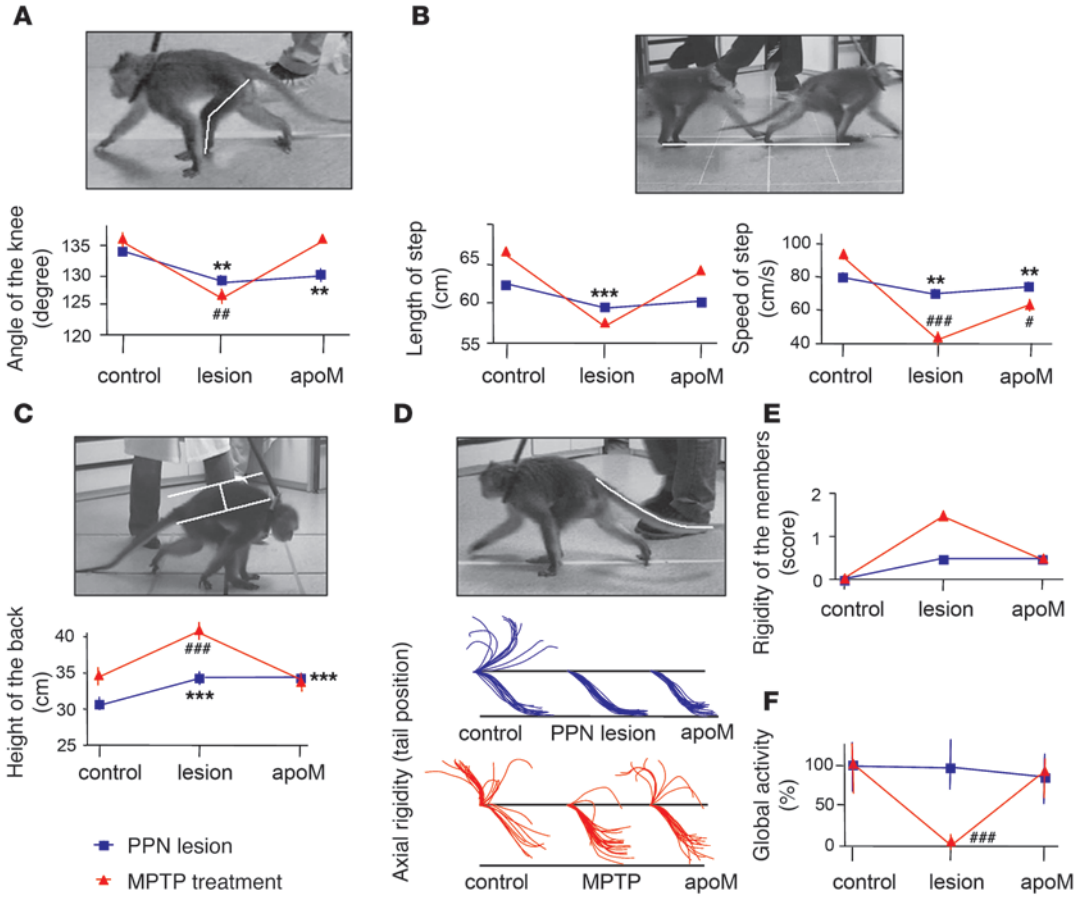

Figure 4

Comparison of MPTP-induced gait and postural disorders with those induced by bilateral cholinergic lesion. Gait and postural parameters were evaluated in macaques (n = 9) in 3 conditions: under control conditions, after bilateral destruction of PPN cholinergic neurons (n = 5) or MPTP intoxication (n = 4), and after apomorphine treatment (apoM). Only results obtained in animal M4, with PPN lesion, and M6, treated by MPTP, are illustrated on the graphs. Symptoms included a decrease in the angle of the knee (**A**) and in step length and speed (**B**), an increase in the height of the back (**C**), modification of the tail position (axial rigidity; **D**), and arm and leg rigidity (**E**). The most prevalent symptom observed after MPTP intoxication was akinesia, as assessed by a dramatic and significant decrease in global activity (**F**). All these symptoms were significantly reversed by apomorphine treatment in MPTP-treated animals, but not in animals with PPN lesion. $^{*}P < 0.05$, $^{**}P < 0.01$, $^{***}P < 0.001$, PPN lesion versus control; $^{\#}P < 0.05$, $^{\#\#}P < 0.01$, $^{\#\#\#}P < 0.001$, MPTP intoxication versus control, Friedman test followed by Wilcoxon test.

Methods

fMRI study

Subjects. We scanned 15 healthy volunteers (7 females and 8 males) with a mean age of 24.7 ± 1.3 years. The study was approved by the local ethics committee, and written informed consent was obtained from all subjects in accordance with the Declaration of Helsinki. All participants were consistent right-handers (Edinburgh Handedness Inventory score, 89.88% ± 2.91%; ref. 39).

Experimental task. For the experimental task, subjects were first familiarized with a corridor with a path in the middle (length, 8 m; width, 2.30 m) and were asked to walk along the path 3 times at a normal speed (1.14 ± 0.10 m/s) and 3 times at around 30% faster (1.49 ± 0.12 m/s). Then, the subjects were shown video recordings of a disc moving in a straight line, at a uniform speed (either normal or faster speed) through the corridor. Subjects then performed a training session. There were 4 conditions: normal IG, faster IG, normal IOM, and faster IOM. For the IG conditions, subjects were asked to imagine walking along the path in a first-person perspective, as if their legs were moving, but without making any actual movements. For the IOM conditions, subjects were asked to vividly evoke a black disc moving along the path, starting from the beginning of the corridor and stopping at the end. During each trial, subjects first saw a photograph of the corridor, with a specific instruction written on it (normal IG, faster IG, normal IOM, faster IOM), projected onto a screen. Once the subjects were ready to start the imagery trial, they were instructed to close their eyes and press a button to signal that they had started imagining walking or seeing the disc moving. Subjects pressed the button again when they imagined that they or the disc had reached the end of the trajectory. A fixation cross was then presented on the screen (intertrial interval, 6–12 s), and the subjects could open their eyes. The training session was performed first outside the scanner (40 trials, 10 per condition), and then inside the MRI scanner (28 trials, 7 per condition). Functional imaging was done immediately after the training session, using an event-related design. Each stimulus presentation was controlled through a PC running Cogent software (Wellcome Department of Imaging Neuroscience). Motor responses (button presses with right thumb) were recorded via an MRI-compatible 1-button stick (Current Designs). The IG and IOM trials (80 trials, 20 per condition) were performed in 2 runs of around 15 minutes each. For each run, the trial order was pseudorandomized across the experimental factors (i.e., IG or IOM and normal or faster speed).

Table 2
Variations in posture and gait parameters after PPN lesion or MPTP intoxication and after apomorphine treatment in macaques

Treatment	Angle of knee	Length of step	Speed of step	Global activity	Back curve	Arm speed	Limb rigidity	Pelvis deviation
PPN lesion (n = 5)								
Lesion	–7%[A]	–7%[A]	–11%[A]	NS	10%[A]	NS	0.7%	0.5%
Apomorphine	–8%[A]	–9%[A]	–17%[A]	NS	15%[A]	X	0.7%	0.5%
MPTP intoxication (n = 4)								
MPTP	NS	–16%[A]	–46%[A]	–87%[A]	27%[A]	138%[A]	1.2%	0%
Apomorphine	NS	NS	–23%[A,B]	–53%[A,B]	NS[B]	NS	0.2%	X

Mean values of parameters of posture and gait were calculated in monkeys with PPN lesion or intoxicated by MPTP, and after subsequent apomorphine treatment in both groups. Effects obtained are expressed as a percentage of the corresponding mean value in controls. Quantity of movement was calculated as described in Methods. The effect of lesion and apomorphine treatment on limb rigidity and pelvis deviation was evaluated on a 0–3 scale and was not statistically compared with the control condition. X, not measured. [A]$P < 0.01$ versus control; [B]$P < 0.01$ versus respective treatment prior to apomorphine, Kruskall-Wallis test followed by Mann-Whitney U test in the event of statistically significant differences.

MRI data collection. Imaging data were collected at the Centre for NeuroImaging Research (CENIR) of Pitié-Salpêtrière Hospital using a Siemens Trio scanner operating at 3 Tesla. T2*-weighted echo-planar images depicting blood oxygenation level–dependent (BOLD) contrast were acquired in a single session (echo time, 30 ms; repetition time, 2.8 s; 40 coronal slices, interleaved acquisition; voxel size, 1.6 × 1.6 × 1.6 mm^3; field of view, 204.8 mm^2). High-resolution anatomical images were acquired using an MPRAGE sequence (echo time, 4.18 ms; repetition time, 2.3 s; 176 sagittal slices; voxel size, 1.0 × 1.0 × 1.0 mm^3; field of view, 256 mm^2).

Data preprocessing. Imaging data were preprocessed with SPM5 statistical parametric mapping software (http://www.fil.ion.ucl.ac.uk/spm) implemented on MATLAB (MathWorks Inc.). Images were corrected for differences in timing of slice acquisition, followed by rigid body motion correction. The motion parameters for translation (x, y, and z) and rotation (yaw, pitch, and roll) were included as covariates of noninterest in the general linear model. Following the coregistration of functional and structural images, the anatomical images were segmented and normalized to stereotactic Montreal Neurological Institute (MNI) space. Functional images were then normalized using the same normalization parameters and smoothed with a 10-mm full width at half-maximum isotropic Gaussian kernel. The time series were high-pass filtered (to a maximum of 1/128 Hz) to remove low-frequency noise. 4 event types were modeled: normal IG, faster IG, normal IOM, and faster IOM. The average hemodynamic response to each event type was modeled using a canonical, synthetic hemodynamic response function (40, 41). Onsets of the events were time-locked to the button press marking the onset of imagery, and duration was set at 0. Regions of significant activation were superimposed on the tracing of cerebral contours in the PPN region, drawn from a 3D histological atlas of the basal ganglia (40, 41) that had been deformed to the MRI template used for the fMRI analyses.

Human postmortem study in PD

The study was performed on brain tissue sections from 8 control individuals, who died without known neurological or psychiatric deficit, and from 12 PD patients. Mean age at death was 85 ± 3 years for controls and 81 ± 3 years for PD patients. Clinical data were retrospectively extracted from patients' charts by 2 raters blinded to the results of stereological quantification of neurons. All PD patients had been treated with L-dopa or dopamine agonists. The diagnosis of PD was made on clinical grounds according to the UKPD Brain Bank Criteria (42) and confirmed postmortem on the basis of neuropathological examination. PD patients were distributed between 2 groups according to the scores for items 29 (balance) and 30 (gait) of the Unified PD Rating Scale (UPDRS; ref. 43) obtained while patients were in the "on" medication state. The range was 0–4, with a higher score indicating a more severe impairment. Patients scoring 2 or higher on one of these items were classified in the group characterized by balance deficits or falls (n = 6). The other patients had no balance deficits or falls (n = 6).

Macaque study

Animals. All experiments were carried out in accordance with the recommendations contained in the European Community Council Directives of 1986 (86/609/EEC) and the NIH Guide for the Care and Use of Laboratory Animals and were approved by the French Animal Ethics Committee of INSERM. The animals were housed under conditions of constant temperature (21°C ± 1°C), humidity (55% ± 5%), and air replacement (16 times/h), on a 12-hour light/12-hour dark cycle with access ad libitum to food and water. In order to quantify the loss of PPN neurons after MPTP treatment, we used brain sections obtained from macaques previously analyzed for another study (35). There were 7 aged macaques (*Macaca arctoides*), estimated to be about 30 years old according to their dentition and the appearance of their hair, and 8 young macaques (*Macaca fascicularis*), aged 3–5 years. The present study also included 5 *M. fascicularis* used for testing the effect of bilateral PPN lesion on gait and posture and 4 *M. fascicularis* intoxicated by MPTP to test the effect of dopaminergic lesions on gait and posture; they were 5–6 years old and their weights ranged from 3 to 5 kg.

Behavioral analysis. We initially habituated 9 macaques to walk guided with a pole in a corridor; this learning period lasted about 2–3 months per animal. The animals were videotaped with orthogonally positioned cameras (face and profile). The animals' right and left sides were both considered. The video recordings were analyzed offline in order to quantify various parameters of gait and posture. For this purpose, images were extracted from the face and profile videos, each image being selected on the basis of the body axis of the animal during the walk sequence, which had to be parallel to a line drawn on the floor, and of the position of its arms and legs, which had to be identical from one image to another. The parameters were the angle of the knee and the elbow; the height of the pelvis (length of the perpendicular straight line between the tail insertion and the line between the 2 feet) and of the back (distance between the line extending from the tail insertion and the top of the neck and the parallel line tangent to the top of the back); the step length (distance between 2 consecutive contacts of the same foot) and speed (step length divided by its duration, estimated from the number of consecutive images between 2 consecutive ground contacts of the same foot); and the tail position. These different parameters were quantified using ImageJ software (http://rsb.info.nih.gov/ij/links.html). Animals were also trained to sit quietly in a primate chair and be manipulated by the examiner to clinically assess rigidity and tremor

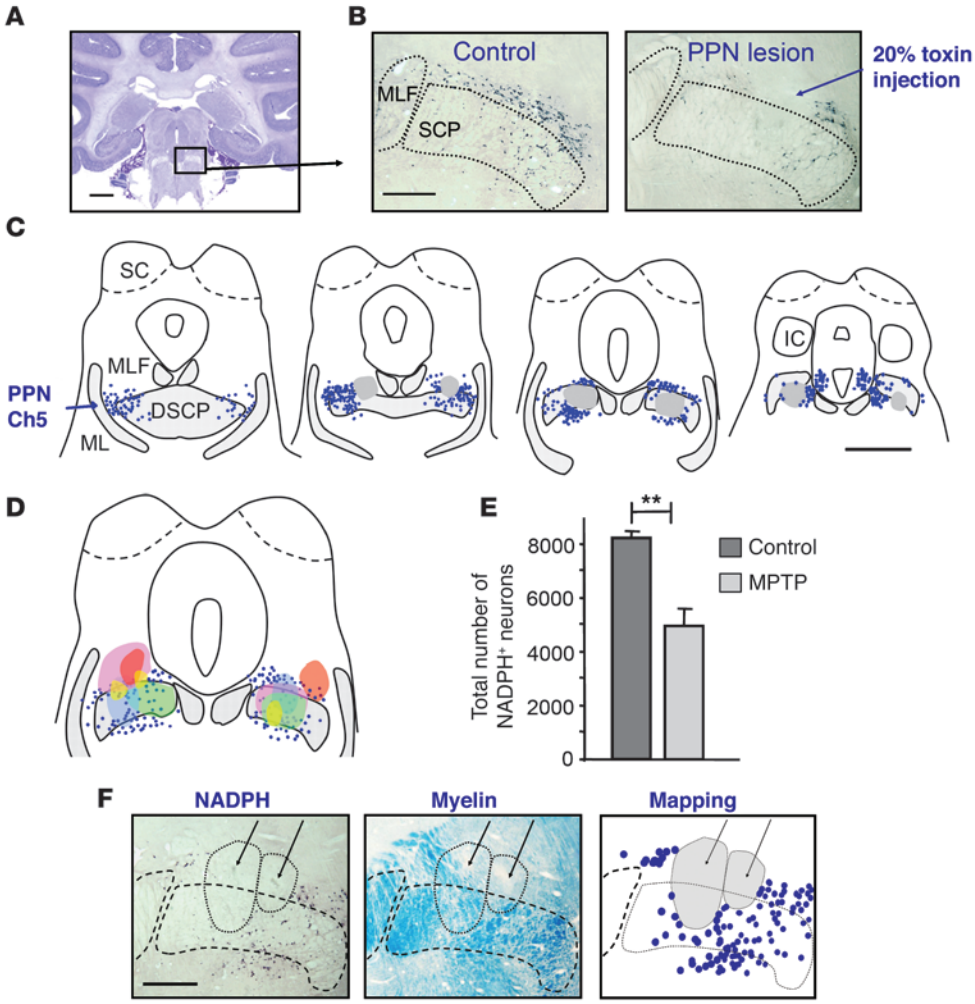

Figure 5

Loss of NADPH+ neurons after bilateral PPN lesion. (**A**) Nissl-stained section showing the anatomical localization of the PPN (boxed region) in a control macaque brainstem. (**B**) Photomicrographs of PPN sections labeled for NADPH diaphorase histochemistry, showing a 20% toxin injection site into the PPN compared with a control. (**C**) Computer-generated maps of NADPH+ neurons (blue) in 4 regularly spaced sections covering the anteroposterior extent of the structure in lesioned animal M4. Each dot represents an NADPH+ neuron; gray areas represent the extent of the injection site; hatched areas denote myelinated nerve fibers. (**D**) All injection sites of the 5 macaques were transferred onto the corresponding brainstem map of macaque M4. Each individual is represented by a different color. Note that the cholinergic part of the PPN was lesioned in all animals. (**E**) Quantification of the total number of NADPH+ neurons in the PPN, showing that neuronal loss reached 39% in lesioned animals ($n = 5$) compared with controls ($n = 5$). $^{**}P < 0.01$, Mann-Whitney *U* test. (**F**) Adjacent PPN sections, labeled for NADPH diaphorase histochemistry and for myelin staining with luxol fast blue, and mapping of NADPH+ neurons showed that myelinated fibers were preserved after toxin injections at 20%. Arrows indicate the center of 2 lesions. IC, inferior colliculus; SCP, superior cerebellar peduncle. Scale bars: 5 mm (**A** and **C**); 1 mm (**B** and **F**).

(rated between 0 and 3). They also learned a simple food retrieval task to study the execution of voluntary movements of the upper arms, during which speed of arm movement was quantified. The task consisted of picking up food pieces placed in wells on a 24-well board. The animals were taught to retrieve the food on the right and left part of the board with their right and left hands, respectively. The motor activity of the macaques was assessed when they were free to move in their home cage and was performed using a video image analyzer system (Vigie Primates ViewPoint). Using this system, the quantity of movement was expressed in arbitrary units and calculated as changes in gray level in pixels from one image to the next, counted every 80 ms for 20 minutes.

MPTP treatment. We used brain sections obtained from 3 aged and 4 young macaques that received MPTP treatment (0.25–0.60 mg/kg) as previously described, and 4 young and 4 aged macaques were used as controls (38). For the present study, we also intoxicated 4 young macaques (*M. fascicularis*) using the same protocol. Parkinsonian symptoms (akinesia, rigidity, postural instability, and intermittent episodes of tremor) were scored on a disability scale of 0–25 (18).

Injection of urotensin II–conjugated diphtheria toxin. PPN lesions were performed on 5 macaques. Animals were tranquilized with ketamine (10 mg/kg) and atropine (0.1 mg/kg) and placed in a stereotactic apparatus, where they were maintained on isoflurane anesthesia (1%–2%). A solution of isotonic saline was given i.v. to maintain fluid levels, and solumedrol (0.2 ml/kg) was administered to preclude brain edema. All surgical procedures were performed aseptically, and recordings of heart rate, respiration patterns, blood pressure, and body temperature were monitored throughout the surgery. Lesion was performed by injecting a urotensin II–conjugated diphtheria toxin locally into the PPN region. This toxin has been developed to specifically kill PPN cholinergic neurons, which have previously been shown to express specifically the urotensin II receptor in rodents (44). The stereotactic injections were guided by radiological visualization of ventricular landmarks (anterior and posterior commissures; ref. 45 and Supplemental Figure 3). A fine needle attached to a 10-μl Hamilton syringe beveled at a 30° angle was used for toxin infusion. Lesions were made by giving 4 infusions per hemisphere (2 depths at 2 anteroposterior locations). Each injection was slowly infused (0.2 μl/min), and the needle was maintained in position for an additional 10-minute period before infusing the next location. Once the injections had been performed, the skin was sutured, and Carprofene (0.1 ml/kg; Vericore Limited) was given for analgesia. The neurotoxin was first stereotaxically injected unilaterally; then, 3–4 weeks later, a contralateral injection was performed using the same procedure. To exclude nonspecific behavioral effects, a sham injection was performed in the right PPN of animal M2 at 2 weeks before the toxin was injected. No behavioral changes were observed under such conditions.

Volume, concentration, and specificity of the toxin. The effective range of toxin was explored in monkey M1. It was found that 10 μl of 3% and 5% doses

(diluted in sterile water and injected at 2 different anteroposterior levels of the same hemisphere) did not produce any postural deficits and resulted in very small lesions of the cholinergic neurons (17% maximum; Supplemental Figure 4A). The 10% dose injected 3 weeks later in the other hemisphere of the same animal induced very slight deficits and small lesions (21% maximum). We thus decided to inject a 30% dose in monkeys M2 and M3 (3 and 10 μl, respectively) and a 20% dose in monkeys M4 and M5 (10 μl). All these injections produced significant behavioral changes and cholinergic neuronal loss. We then tested the specificity of the toxin and estimated the loss of noncholinergic neurons on adjacent sections labeled for NADPH diaphorase and a marker of neuronal cell bodies (NeuN; Supplemental Figure 4B). Whatever the concentration used, some $NeuN^+$ neurons remained at the periphery of the injection site, where 100% of cholinergic neurons were lost. The higher the concentration, the greater the loss of noncholinergic neurons observed (Supplemental Figure 4C). In conclusion, the toxin preferentially, but not exclusively, destroyed cholinergic neurons.

Apomorphine treatment in young macaques. Apomorphine (120 μg/kg; Aguettent) was given i.m. after PPN lesion or MPTP intoxication (2–3 weeks after the surgery or the last MPTP injection when symptoms reached a maximum level of severity) in order to test whether the behavioral changes induced by the lesion are dopamine-resistant symptoms.

Histochemistry

All macaques were deeply anesthetized and intracardially perfused with 4% paraformaldehyde in PBS. Brains were removed, immersed in 30% sucrose in PBS, and frozen. Transverse sections 50 μm thick were cut on a freezing microtome and stored at 4°C in PBS containing sodium azide until immunohistochemical analysis.

Series of regularly interspaced (500 μm apart) sections of macaque brains were processed for NADPH diaphorase histochemistry as previously described (46). Some sections were counterstained with neural red or Cresyl violet. Other series of free-floating sections used for immunohistochemistry were incubated in the antibodies mouse anti-TH (1:5,000; Immunostar) or mouse anti-NeuN (1:500; Chemicon) at 4°C for 2 days. They were then incubated in peroxidase-conjugated anti-mouse secondary antibody. The antibodies were visualized by peroxidase histochemistry with diaminobenzidine as substrate (Vector Labs). Some sections were also stained with luxol fast blue to label myelinated fibers. In order to analyze the microglial activation, series of sections were also stained for HLA-DR (α chain, 1:50 monoclonal antibody; Dako) as previously described (47).

After autopsy, the human brains were halved sagittally, and one half was dissected into smaller blocks of tissue and fixed in 4% paraformaldehyde and 15% picric acid as previously described (43). Regularly interspaced free-floating 40-μm frozen transverse sections of the PPN (every 720 μm) were then processed for histochemical detection of AChE (48) and counterstained with cresyl violet.

Data analysis

The criteria used to delineate the boundaries of the PPN have been described previously (46). The number of $AChE^+$ neurons in humans and the number of $NADPH^+$ neurons in macaques were counted on 5 regularly interspaced PPN sections covering the anteroposterior extent of the structure. The sections were matched anatomically in each of the brains, while verifying that the cross-sections of the PPN were similar in all individuals. The extent of dopaminergic denervation in PD patients was assessed by counting TH^+ neurons on 8 regularly interspaced nigral sections (every 1,440 μm) using the same method. Estimation of the total number of cholinergic and dopaminergic neurons was performed using a semiautomatic stereology system with a computer-based system (Mercator; ExploraNova). The number of Nissl-stained noncholinergic neurons in the cuneiform nucleus, and of $HLA\text{-}DR^+$ cells in the PPN, was counted using the same stereological method and expressed as the number of cells per cubic millimeter. In MPTP-treated macaques, the density of TH^+ immunoreactivity was quantified in the striatum by measuring the optical density under brightfield illumination, as previously described (49).

Statistics

For fMRI analysis, a paired *t* test was used to determine whether means from the healthy subject group varied over 2 test conditions: IG versus IOM and normal versus fast walking speed. Parameter estimates for IG and IOM at normal and faster speed were determined using planned contrasts. The linear combinations of parameter estimates for each contrast were stored as separate images for each subject. These contrast images were entered into a 1-sample *t* test, to permit inferences about condition effects across subjects that generalize to the population (i.e., a random-effects analysis). These contrasts produced statistical parametric maps (SPMs) of the *t* statistics at each voxel. Considering our a priori hypothesis regarding the involvement of the PPN region in IG versus IOM comparisons (including both normal and faster speed) and in faster versus normal IG, and given the small size of the structure, contrasts were thresholded with a *P* value of 0.001, uncorrected for multiple comparisons, unless stated otherwise. Only activations involving contiguous clusters of at least 30 voxels were interpreted.

A Kruskall-Wallis test followed by a Mann-Whitney *U* test was used to compare neuronal loss in 3 groups (faller PD, nonfaller PD, and control), and a Mann-Whitney *U* test alone was used to determine whether a difference existed between 2 groups of individuals.

The walk of each macaque was analyzed from 3–5 video sequences taken in 3 conditions: control, after PPN or dopaminergic lesion, and after apomorphine injection. For each animal, 25 images were extracted from frontal video, and 25 other images from profile video, each image being selected on the basis of the body axis of the animal during the walk sequence as described above. The mean values of each parameter were then calculated for a given individual, and a Friedman test was then used to analyze the differences among the 3 conditions, followed by a Wilcoxon paired-sample test in the event of statistically significant differences. The mean values of parameters calculated for a given animal were also expressed as a percentage in 5 monkeys with PPN lesion and after apomorphine treatment, and in 4 monkeys intoxicated by MPTP and after apomorphine treatment. A Kruskall-Wallis test was then used to analyze variance among the 3 conditions, followed by a Mann-Whitney *U* test in the event of statistically significant differences. The effect of lesion and apomorphine treatment on the limb rigidity and pelvis deviation parameters was evaluated on a scale of 0–3 and was not statistically compared with the control condition. All data are presented as mean ± SEM. A value of $P < 0.05$ was considered to be statistically significant, except for fMRI data ($P < 0.001$).

Acknowledgments

This study was supported by INSERM, the Fondation de l'Avenir, and the Michael J. Fox Foundation. We would like to thank Eric Bertasi and Romain Valabregue for performing fMRI in healthy humans and Nick Barton for language editing.

Received for publication February 11, 2010, and accepted in revised form May 26, 2010.

Address correspondence to: Chantal François or Etienne C. Hirsch, GH Pitié Salpêtrière, 4ème étage, 47 Boulevard de l'Hôpital, 75651 Paris Cedex 13, France. Phone: 33.1.42.16.00.68; Fax: 33.1.45.82.88.93; E-mail: chantal.francois@upmc.fr (C. François). Phone: 33.1.42.16.22.02; Fax: 33.1.44.24.36.58; E-mail: Etienne.hirsch@upmc.fr (E.C. Hirsch).

1. Bloem BR, Hausdorff JM, Visser JE, Giladi N. Falls and freezing of gait in Parkinson's disease: a review of two interconnected, episodic phenomena. *Mov Disord*. 2004;19(8):871–884.
2. Garcia–Rill E. The pedunculopontine nucleus. *Prog Neurobiol*. 1991;36(5):363–389.
3. Mesulam MM, Mufson EJ, Levey AI, Wainer BH. Atlas of cholinergic neurons in the forebrain and upper brainstem of the macaque based on monoclonal choline acetyltransferase immunohistochemistry and acetylcholinesterase histochemistry. *Neuroscience*. 1984;12(3):669–686.
4. Jahn K, et al. Imaging human supraspinal locomotor centers in brainstem and cerebellum. *NeuroImage*. 2008;39(2):786–792.
5. Bakker M, et al. Motor imagery of foot dorsiflexion and gait: effects on corticospinal excitability. *Clin Neurophysiol*. 2008;119(11):2519–2527.
6. Iseki K, Hanakawa T, Shinozaki J, Nankaku M, Fukuyama H. Neural mechanisms involved in mental imagery and observation of gait. *NeuroImage*. 2008;41(3):1021–1031.
7. Hirsch EC, Orieux G, Muriel MP, Francois C, Feger J. Nondopaminergic neurons in Parkinson's disease. *Adv Neurol*. 2003;91:29–37.
8. Zweig RM, Jankel WR, Hedreen JC, Mayeux R, Price DL. The pedunculopontine nucleus in Parkinson's disease. *Ann Neurol*. 1989;26(1):41–46.
9. Pahapill PA, Lozano AM. The pedunculopontine nucleus and Parkinson's disease. *Brain*. 2000; 123(pt 9):1767–1783.
10. Plaha P, Gill SS. Bilateral deep brain stimulation of the pedunculopontine nucleus for Parkinson's disease. *NeuroReport*. 2005;16(17):1883–1887.
11. Stefani A, et al. Bilateral deep brain stimulation of the pedunculopontine and subthalamic nuclei in severe Parkinson's disease. *Brain*. 2007; 130(pt 6):1596–1607.
12. Zrinzo L, et al. Stereotactic localization of the human pedunculopontine nucleus: atlas-based coordinates and validation of a magnetic resonance imaging protocol for direct localization. *Brain*. 2008;131(pt 6):1588–1598.
13. Ferraye MU, et al. Effects of pedunculopontine nucleus area stimulation on gait disorders in Parkinson's disease. *Brain*. 2010;133(pt 1):205–214.
14. Moro E, et al. Unilateral pedunculopontine stimulation improves falls in Parkinson's disease. *Brain*. 2010;133(pt 1):215–224.
15. Piallat B, et al. Gait is associated with an increase in tonic firing of the sub-cuneiform nucleus neurons. *Neuroscience*. 2009;158(4):1201–1205.
16. Herrero MT, Hirsch EC, Javoy–Agid F, Obeso JA, Agid Y. Differential vulnerability to 1–methyl–4–phenyl–1,2,3,6–tetrahydropyridine of dopaminergic and cholinergic neurons in the monkey mesopontine tegmentum. *Brain Res*. 1993; 624(1–2):281–285.
17. Heise CE, Teo ZC, Wallace BA, Ashkan K, Benabid AL, Mitrofanis J. Cell survival patterns in the pedunculopontine tegmental nucleus of methyl-4-phenyl-1,2,3,6-tetrahydropyridine-treated monkeys and 6OHDA-lesioned rats: evidence for differences to idiopathic Parkinson disease patients? *Anat Embryol (Berl)*. 2005;210(4):287–302.
18. Luquin MR, et al. Recovery of chronic parkinsonian monkeys by autotransplants of carotid body cell aggregates into putamen. *Neuron*. 1999;22(4):743–750.
19. Ovadia A, Zhang Z, Gash DM. Increased susceptibility to MPTP toxicity in middle-aged rhesus monkeys. *Neurobiol Aging*. 1995;16(6):931–937.
20. Shik ML, Severin FV, Orlovskii GN. Control of walking and running by means of electric stimulation of the midbrain. *Biofizika*. 1966;11(4):659–666.
21. Takakusaki K, Habaguchi T, Ohtinata-Sugimoto J, Saitoh K, Sakamoto T. Basal ganglia efferents to the brainstem centers controlling postural muscle tone and locomotion: a new concept for understanding motor disorders in basal ganglia dysfunction. *Neuroscience*. 2003;119(1):293–308.
22. Grillner S. Control of locomotion in bipeds, tetrapods and fish. In: Brooks VB, ed. *Handbook of Physiology - the nervous system II*. Baltimore, Maryland, USA: American Physiological Society; 1981:1199–1236.
23. Winn P. Experimental studies of pedunculopontine functions: are they motor, sensory or integrative? *Parkinsonism Relat Disord*. 2008;14 suppl 2:S194–S198.
24. Inglis WL, Winn P. The pedunculopontine tegmental nucleus: Where the striatum meets the reticular formation. *Prog Neurobiol*. 1995;47(1):1–29.
25. Inglis WL, Olmstead MC, Robbins TW. Selective deficits in attentional performance on the 5-choice serial reaction time task following pedunculopontine tegmental nucleus lesions. *Behav Brain Res*. 2001;123(2):117–131.
26. Alderson HL, Latimer MP, Winn P. A functional dissociation of the anterior and posterior pedunculopontine tegmental nucleus: excitotoxic lesions have differential effects on locomotion and the response to nicotine. *Brain Struct Funct*. 2008;213(1–2):247–253.
27. Munro-Davies LE, Winter J, Aziz TZ, Stein JF. The role of the pedunculopontine region in basal-ganglia mechanisms of akinesia. *Exp Brain Res*. 1999;129(4):511–517.
28. Kojima J, et al. Excitotoxic lesions of the pedunculopontine tegmental nucleus produce contralateral hemiparkinsonism in the monkey. *Neurosci Lett*. 1997;226(2):111–114.
29. Matsumura M, Yamaji Y. The role of the pedunculopontine tegmental nucleus in experimental parkinsonism in primates. *Stereotact Funct Neurosurg*. 2001;77(1–4):108–115.
30. Winn P, Stone TW, Latimer M, Hastings MH, Clark AJ. A comparison of excitotoxic lesions of the basal forebrain by kainate, quinolinate, ibotenate, N-methyl-D-aspartate or quisqualate, and the effects on toxicity of 2-amino-5-phosphonovaleric acid and kynurenic acid in the rat. *Br J Pharmacol*. 1991;102(4):904–908.
31. Haaland KY, Harrington DL. Hemispheric asymmetry of movement. *Curr Opin Neurobiol*. 1996; 6(6):796–800.
32. Sacco K, Cauda F, Cerliani L, Mate D, Duca S, Geminiani GC. Motor imagery of walking following training in locomotor attention. The effect of 'the tango lesson'. *NeuroImage*. 2006;32(3):1441–1449.
33. Rinne JO, Ma SY, Lee MS, Collan Y, Roytta M. Loss of cholinergic neurons in the pedunculopontine nucleus in Parkinson's disease is related to disability of the patients. *Parkinsonism Relat Disord*. 2008;14(7):553–557.
34. Zhang JH, Sampogna S, Morales FR, Chase MH. Age-related changes in cholinergic neurons in the laterodorsal and the pedunculo-pontine tegmental nuclei of cats: a combined light and electron microscopic study. *Brain Res*. 2005;1052(1):47–55.
35. George O, et al. Smad-dependent alterations of PPT cholinergic neurons as a pathophysiological mechanism of age-related sleep-dependent memory impairments. *Neurobiol Aging*. 2006;27(12):1848–1858.
36. Sheffield L, Berman NE. Microglial expression of MHC class II increases in normal aging of nonhuman primates. *Neurobiol Aging*. 1998;19(1):47–55.
37. Lavoie B, Parent A. Pedunculopontine nucleus in the squirrel monkey: cholinergic and glutamatergic projections to the substantia nigra. *J Comp Neurol*. 1994;344(2):232–241.
38. Rolland AS, et al. Evidence for a dopaminergic innervation of the pedunculopontine nucleus in monkeys, and its drastic reduction after MPTP intoxication. *J Neurochem*. 2009;110(4):1321–1329.
39. Oldfield RC. The assessment and analysis of handedness: the Edinburgh inventory. *Neuropsychologia*. 1971;9(1):97–113.
40. Friston KJ, et al. Event-related fMRI: characterizing differential responses. *NeuroImage*. 1998;7(1):30–40.
41. Friston KJ, Josephs O, Rees G, Turner R. Nonlinear event-related responses in fMRI. *Magn Reson Med*. 1998;39(1):41–52.
42. Hughes AJ, Daniel SE, Kilford L, Lees AJ. Accuracy of clinical diagnosis of idiopathic Parkinson's disease: a clinico-pathological study of 100 cases. *J Neurol Neurosurg Psychiatry*. 1992;55(3):181–184.
43. Fahn S. Concept and classification of dystonia. *Adv Neurol*. 1998;50:1–8.
44. Clark SD, et al. Fusion of diphtheria toxin and urotensin II produces a neurotoxin selective for cholinergic neurons in the rat mesopontine tegmentum. *J Neurochem*. 2007;102(1):112–120.
45. Percheron G, Yelnik J, François C. Systems of coordinates for stereotactic surgery and cerebral cartography: advantages of ventricular systems in monkeys. *J Neurosci Methods*. 1986;17(2–3):69–88.
46. Hirsch EC, Graybiel AM, Duyckaerts C, Javoy–Agid F. Neuronal loss in the pedunculopontine tegmental nucleus in Parkinson disease and in progressive supranuclear palsy. *Proc Natl Acad Sci U S A*. 1987;84(16):5976–5980.
47. Barcia C, et al. Evidence of active microglia in substantia nigra pars compacta of parkinsonian monkeys 1 year after MPTP exposure. *Glia*. 2004;46(4):402–409.
48. Graybiel AM, Hirsch EC, Agid YA. Differences in tyrosine hydroxylase-like immunoreactivity characterize the mesostriatal innervation of striosomes and extrastriosomal matrix at maturity. *Proc Natl Acad Sci U S A*. 1987;84(1):303–307.
49. Jan C, et al. Quantitative analysis of dopaminergic loss in relation to functional territories in MPTP-treated monkeys. *Eur J Neurosci*. 2003;18(7):2082–2086.